INSTITUTE OF PHYSICS PUBLISHING JOURNAL OF OPTICS A: PURE AND APPLIED OPTICS

J. Opt. A: Pure Appl. Opt. **5** (2003) 159–162 PII: S1464-4258(03)57413-X

Optimal design of broadened flat bandpass electro-optic phase modulator based on aperiodic domain-inverted grating

Xianfeng Chen, Xianglong Zeng, Yuping Chen, Yuxing Xia and Yingli Chen

Institute of Optics and Photonics, Department of Applied Physics, Shanghai Jiaotong University, Shanghai 200240, People's Republic of China

Received 11 December 2002
Published 10 March 2003
Online at stacks.iop.org/JOptA/5/159

Abstract
A new optimization approach for the design of an integrated bandpass travelling-wave modulator based on an aperiodic domain-inverted grating is presented. The flat, broad bandpass frequency responses of 10 and 20 GHz (0.5 dB) centred at 200 GHz are demonstrated. The sequences and the length of the domains are optimized to realize the pre-designed wide, flat frequency response over the required frequency range by use of the simulated annealing method. The physical mechanism for this kind of modulator is attributed to the constructive interference effect of the overall domains.

Keywords: Simulated annealing (SA) method, domain-inverted grating, travelling-wave modulator

1. Introduction

Driven by the demand for wideband optical communication systems and high-speed pulse processing systems, a broadband and flat frequency response at high frequency is expected in electro-optic modulators (EOMs). Due to phase velocity mismatch between the microwave signal and the optical wave [1], high driver frequency modulation is limited. Recently the concept of a phase reversal electrode and domain inverted structures was introduced to overcome this problem [2, 3]. In an attempt to extend the bandwidth response, electrode patterns [4] or domains based on 13-bit Barker codes [3, 4] and steplike phase reversal [5] of aperiodic structures were demonstrated experimentally. Zolotov *et al* [6] put forward a chirped-toothed electrode structure with triangular or trapezoidal edges, which showed perfect uniform frequency response.

However, as the modulation frequency of travelling-wave modulators increases, the length of the phase reversal of those electrodes, as shown in figure 1(a), must be shortened. As a result, the configuration of the electrodes becomes complicated and the overlap between the optical and microwave fields is poor [7], and 13-bit maximal Barker code length or few-section phase reversal limits further bandwidth broadening. The optimum algorithm [5] becomes difficult when the number of sections increases.

As an alternative approach, a domain-inverted grating, such as periodically poled $LiNbO_3$ (PPLN) and periodically poled $LiTaO_3$ (PPLT), can realize quasi-velocity matching in EOMs [8]. Just like the nonlinear optical coefficient, the electro-optic coefficient also has different signs in different domains. In essence, the modulation for the electro-optic coefficient has the same effect as the modulation for the direction of the applied field in the waveguide. With the maturing of the electric-poling technique [12], the period of the modulation can be as small as a few microns.

In this paper, we propose, for the first time to the best of our knowledge, an approach to obtain a wide, flat bandwidth at high frequency EOM based on an aperiodic domain-inverted grating. It is constructed with opposite ferroelectric domains, whose lengths are less than the coherence length. The simulated annealing (SA) method [10] is applied to optimize the identical efficiency of modulation over the required frequency range. The width of each individual domain in figure 1 may be different. The configuration of electrodes takes advantage of that of the simpler travelling-wave modulators, which tolerates the errors of the fabrication

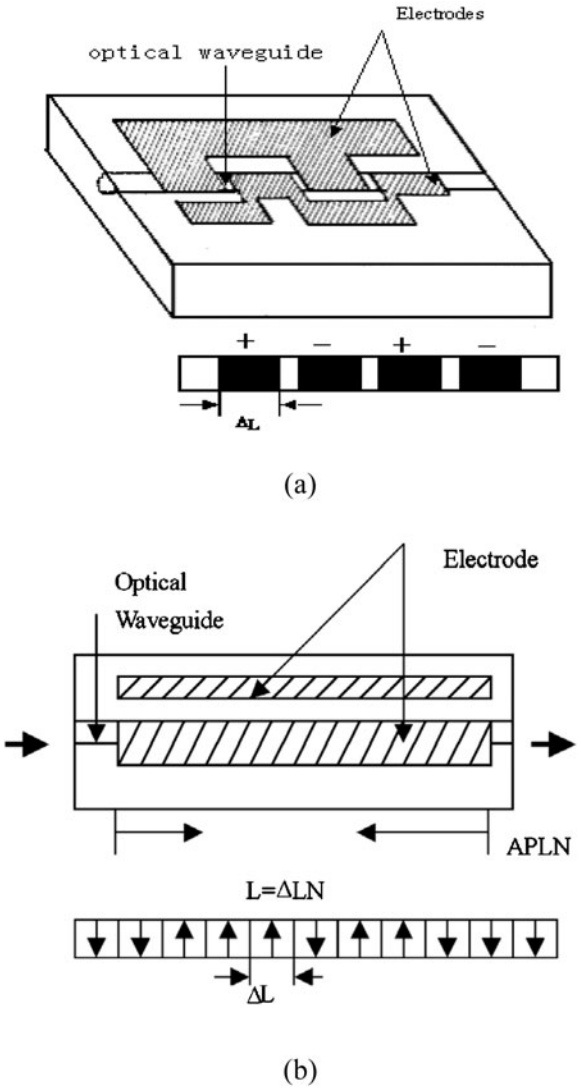

Figure 1. (a) The configuration of periodic phase reversal electrodes. (b) Model of the travelling-wave modulator and the aperiodic domains in part; the sign of the electro-optic coefficient changes with the domain orientation.

processes. The impedance calculation is also simplified. By locating the relative position between the waveguide zone and the electrodes, the overlap integral can be maximized. It is shown that by choice of an appropriate configuration of the domain-inverted structure, velocity matching can be achieved at the pre-designed high frequency with a broadened flat bandwidth frequency response over the required frequency range.

2. Model of travelling-wave modulator

Figure 1(b) shows the schematic diagram of a phase modulator with an aperiodic domain-inverted grating; the length of the optical waveguide L is uniformly divided into an integer number of building blocks ΔL, to be arbitrarily assigned either polarity. The total length of the sample is $L = \Delta LN$. This structure can be fabricated by the room-temperature electric-poling technique with pre-designed mask patterns. The sign of the electro-optic coefficient r_{33} in the blocks is inversed according to the different domain orientation, which is the same as that of the nonlinear coefficient d_{33}. Different numbers of adjacent blocks with the same orientation are bunched in the positive or negative domains. The domain sequence is determined by means of SA methods. In terms of the characteristic structure, the arrangement of the domains is irregular.

The frequency response of this kind of modulator is derived in terms of the normalized phase shift $\phi(f_m)/FL$, given by [2, 9]

$$\frac{\phi(f_m)}{FL} = \frac{1}{L}\int_0^L \Gamma(z)g(z)\exp[-\gamma(f_m)z]\,\mathrm{d}z \qquad (1)$$

where the excitation function $F = (-n_o^3 r E_m \pi/\lambda)\exp(\mathrm{j}2\pi f t_0)$, and the overlap integral $\Gamma(z)$, which measures the degree of the overlapping between the microwave field and the optical field, is given by

$$\Gamma(z) = \frac{G}{V}\frac{\iint E_m(x,y)[\varepsilon(x,y)]^2\,\mathrm{d}x\,\mathrm{d}y}{\iint[\varepsilon(x,y)]^2\,\mathrm{d}x\,\mathrm{d}y} = \text{constant}. \qquad (2)$$

$E_m(x, y)$ is the transverse electric field distribution of the microwave and $\varepsilon(x, y)$ is the transverse electric field of the optical wave. f and f_m are the optical frequency and the microwave frequency respectively. G is the gap between two electrodes and V is the applied voltage. L is the total length of the electrode. For the configuration of the electrodes described above, it is clear that the overlap integrals are the same along the waveguide. It can also be maximized by the appropriate relative locations of the waveguide and the electrodes. r is the electro-optical coefficient of the crystal. $g(z) = r(z)/r$ is the normalized structure function, which can now be described by the finite sequence of binary values of ± 1, corresponding to the block orientation. n_o is the refractive index of the optical wave. E_m is the amplitude of the microwave modulating electric field; λ is the optical wavelength; $\gamma = \alpha + \mathrm{j}\beta'$ is the propagation constant of the microwave field; α is the attenuation coefficient; if the microwave loss is negligible, it is zero. β' is the microwave phase constant; n_m is the refractive index for the modulating microwave; c is the velocity of light in free space. The normalized phase shift can be reduced to

$$\begin{aligned} G(f_m) &= \left|\frac{\phi(f_m)}{FL}\right| = \left|\frac{\Gamma}{L}\int_0^L \mathrm{d}z\,\mathrm{e}^{-\alpha z - \mathrm{j}\beta' z} g(z)\right| \\ &= \frac{\Gamma}{N}\left|\sin c\left(\frac{\Delta L}{L_c(f_m)}\right)\right| \\ &\quad \times \left|\left\{\sum_{q=0}^{N-1} g(z_q)\mathrm{e}^{-\alpha(q+0.5)\Delta L}\mathrm{e}^{-\mathrm{j}[\pi(q+0.5)\Delta L/L_c(f_m)]}\right\}\right| \end{aligned} \qquad (3)$$

where $L_c(f_m) = \frac{2\pi}{\beta'} = \frac{c}{f_m(n_m - n_o)}$ is the coherence length. It is clearly seen that the normalized phase shift is the Fourier transform of the normalized structure function $g(z)$ [4, 6] and the frequency response of the travelling-wave modulator is the spectrum function in the microwave frequency domain. By perturbing the periodic structure function $g(z)$ the spectral components in the frequency domain can spread to the wings from the main lobe. The second factor in equation (3) is determined by the interference effect of overall domains, which is globally dependent on the sequences and the sign of every domain. The optimization problem at hand is how to determine the domain structure function.

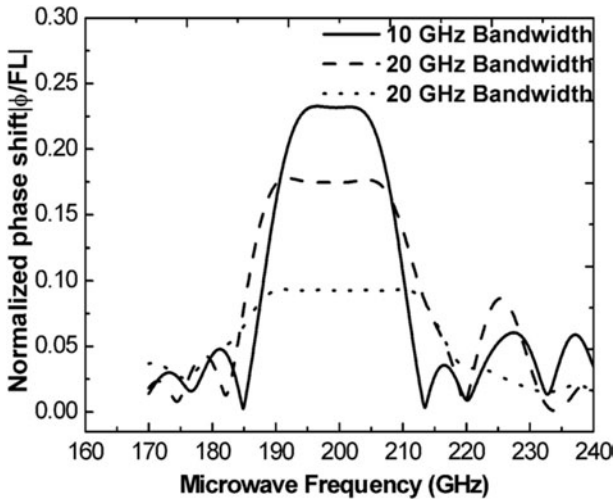

Figure 2. Calculated broadened bandwidth with flat frequency response for the aperiodic grating constructed by the specified sequence: dashed curve for microwave frequency-dependent loss $\alpha_0 = 0.1$ dB cm^{-1} GHz$^{-0.5}$ at 20 GHz pre-designed bandwidth.

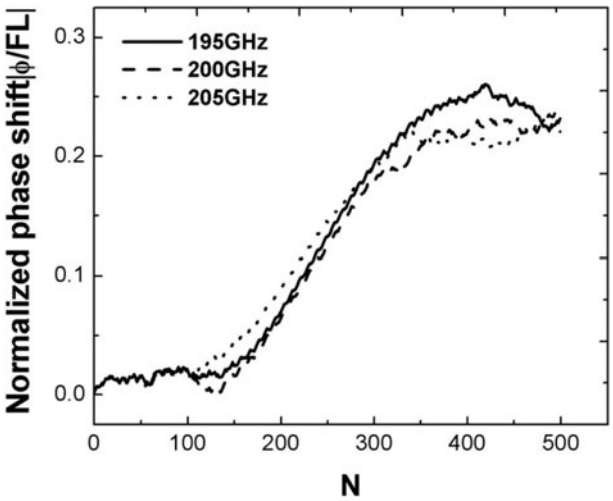

Figure 3. The normalized phase shift versus the block number N along the propagation direction. The modulated frequencies chosen for calculation are within the bandwidth shown in figure 2.

3. Modulator response

In all modulators that we have modelled, we assume the use of a coplanar transmission-line configuration similar to that of figure 1, and adopt that the total length of the waveguide L is 20 mm and $N = 500$. Although the length of each block $\Delta L = 20\,\text{mm}/500 = 40\ \mu$m is far smaller than the coherence length, it can easily fabricated with high accuracy in the state of the art of the electric-poling technique [11].

For z-cut $LiNbO_3$, the typical effective microwave index is 4.225 and the guided optical index is 2.138 at 1.5 μm wavelength [9]. To obtain a flat frequency response over a specified frequency range f_1–f_2, it is required to minimize its variation over the frequency range. The object function in the SA method is chosen as

$$E = \beta\left[\sum_{\alpha}\left|G_0 - G_\alpha(f_m)\right|\right] + \varepsilon F \tag{4}$$

where G_0 is a pre-designed value in the SA procedure; in this case, we select ten microwave frequencies, which are distributed uniformly over the required frequency range. The normalized variance of the response F is used as a minimization parameter and is given by [12]

$$F = \frac{(f_2 - f_1)\int_{f_1}^{f_f}\left|G(f_m)\right|^2 \mathrm{d}f}{[\int_{f_1}^{f_2}\left|G(f_m)\right|\mathrm{d}f]^2} - 1. \tag{5}$$

So the normalized variance of the response F is taken into our objective function. β and ε are adjustable parameters, which function as the weights of two parts of equation (4) respectively. It is very important to choose the appropriate values of β and ε to obtain a bandpass broadened and flat frequency response in the calculation.

The bandwidth is pre-designed as 10 GHz centred at 200 GHz. The optimal consecutive order of domains is obtained by choice of the appropriate objective function in the SA method. We scan this modulator with use of the sampling frequency from 170 to 240 GHz with a step of 0.1 GHz. The calculation results are shown in figure 2. With the optimized aperiodic structure, the flattop response of pre-designed bandwidth of frequency is achieved only at the expense of the output phase shift.

With the same parameters, other preset bandwidths like 20 GHz (0.5 dB) centred at 200 GHz are also shown in figure 2. The frequency-dependent loss function $\alpha = \alpha_0\sqrt{f}$, and the microwave loss coefficient of $\alpha_0 = 0.1$ dB cm^{-1} GHz$^{-0.5}$, are applied to equation (3). The same 20 GHz pre-designed bandwidth is obtained. The normalized phase shift decreases as the bandwidth is broadened. This is because of the trade-off between the wide bandwidth and the peak value of the normalized phase shift. From the above discussion, the wide bandwidth can be tailored in an aperiodic domain-inverted grating.

It is interesting to investigate the property of the performance of the wide bandwidth as the normalized phase shift changes along the aperiodic grating. The result is shown in figure 3. From the plot, each curve tends to the same point through different paths. This clearly manifests that the wavelengths in a wide bandwidth can all globally be velocity matched by the interference effect of all constructed domains, but undergo different interference processes.

This kind of domain reversal is essentially an aperiodic structure like Baker codes. Some results of Baker codes, such as the improvement of the ratio of the bandwidth to the half-wave voltage (BVR), are similar [2, 5]. But the phase frequency response of the modulator is non-linear, which would degrade the time performance and result in eye closure. Such modulators are suitable for pulse applications [4]. The literature [2, 4, 13] has detailed the nonlinear phase response.

4. Discussion

The emphasis in this paper has focused on the design of pre-designed broadband response at high frequencies, not merely at 200 GHz. An analysis of the operation of travelling-wave modulators with an aperiodic domain-inverted grating has been presented. The use of this aperiodic domain-inverted

grating may lead to spectacular performance for the bandpass broadened and flat response over the required frequency range. The SA method is taken effectively to choose the optimum sequence of the domains. Another optimal method such as genetic algorithms (GAs) can be applied. Compared with conventional modulators that have a uniform or non-periodic (Barker code) electrode pattern, the ripple of the frequency response is greatly reduced, and the simple configuration of the travelling-wave modulator makes the overlap integrals larger, which results in a lower driver voltage. The aperiodic domain-inverted grating can implement a pre-designed flat response with the optimum sequence of the orientation of each block by the SA method, and it would be a promising approach for novel broadband nonlinear optical devices.

Acknowledgments

This research is supported by the Fund of Technological Development in Shanghai, People's Republic of China, under grant No 00JC14027, and the National Science Foundation of China under grant No 60007001.

References

[1] Alferness R C 1982 *IEEE Trans. Microwave Theory Tech.* **30** 1121–37
[2] Erasme D and Wilson M G F 1986 *Opt. Quantum Electron.* **18** 203–11
[3] Wang W, Tavlykaev R and Ramaswamy R V 1997 *IEEE Photon. Technol. Lett.* **9** 610
[4] Nazarathy M, Dolfi D W and Jugerman R L 1987 *J. Opt. Soc. Am.* **4** 1071–9
[5] Hui K W, Wu B Y, Choi Y M, Peng J H and Chiang K S 1997 *IEEE Trans. Microwave Theory Tech.* **45** 142–5
[6] Zolotov E M, Pelekhatyi V M and Tavlykaev R F 1990 *Int. J. Optoelectron.* **5** 503
[7] Hui K W, Chiang K S, Wu B Y and Zhang Z H 1998 *J. Lightwave Technol.* **16** 232
[8] Lu Y Q, Xiao M and Salamo G J 2001 *Appl. Phys. Lett.* **8** 1035
[9] Alferness R C, Korotky S K and Marcatili E A 1984 *IEEE J. Quantum Electron.* **20** 301–9
[10] Kirkpatrick, Gelatt C D and Vecchi M P 1983 *Science* **220** 671
[11] Myers L E, Eckardt R C, Fejer M M, Byer L, Bosenberg R and Pierce J W 1995 *J. Opt. Soc. Am.* B **12** 2102–15
[12] Erasme D, Humphreys D A and Wilson M G F 1998 *J. Lightwave Technol.* **6** 933
[13] Erasme D and Wilson M G F 1986 *Electron. Lett.* **22** 1024